Continuum description of noiseless diffusion-limited aggregation

Klaus Kassner[1] and Efim Brener[2]
[1]*Institut für Festkörperforschung des Forschungszentrums Jülich, 52425 Jülich, Germany*
[2]*Institute for Solid State Physics, Chernogolovka, Russia*
(Received 19 April 1994)

We develop a continuum theory for the compact-growth phase of noise-reduced diffusion-limited aggregation (DLA). Its essential feature is a *dynamic* argument determining the selected growth velocity of the cluster arm tips. With one additional assumption, a parameter-free description is obtained. This description agrees well with the overall shape of numerically simulated clusters, containing up to several tens of thousands of particles. It also provides decent predictions for the step sequences on the cluster arms and for the numerical value of the tip growth probability. Finally, this theory demonstrates that noise-reduced DLA and viscous fingering, having different growth exponents, belong in two different universality classes.

PACS number(s): 68.70.+w, 61.43.Hv, 68.10.−m

Diffusion-limited aggregation (DLA) [1,2] has become a paradigm for fractal growth processes over the years, mostly because it can be easily investigated numerically while giving rise to nontrivial scaling properties of the growing cluster. Nevertheless, our analytic understanding of DLA and related growth models remains limited so far [3,4]. This situation has led to various simplifications of the model such as the introduction of noise reduction [5,6] and of branchless DLA [7,8], which were then studied analytically on varying levels of sophistication [9–12].

Recently, Almgren, Dai, and Hakim presented an analytic theory for the scaling behavior of anisotropic Hele-Shaw flow [13], i.e., viscous fingering. This important work has already become an essential ingredient of an analytic theory describing the entire needle crystal in three-dimensional dendritic growth [14]. We will now employ it to set up a parameter-free continuum theory of DLA in the zero-noise limit.

Almgren *et al.* consider Laplacian growth with constant-flux boundary conditions at infinity and with fourfold anisotropy of the surface tension. Assuming that a four-petal structure evolves whose arm lengths scale with time as $x \sim A\,t^{\alpha}$, they conclude that the arm widths must scale as $y \sim A' t^{1-\alpha}$ (which restricts the growth exponents to $\frac{1}{2} < \alpha < 1$). They then approximate the growth rate on the arms by that of a four-spoke model [15]:

$$\frac{dy}{dt} = B\frac{x}{\sqrt{x_{tip}^4 - x^4}}\,, \tag{1}$$

which allows one to immediately derive an expression for the full finger shape

$$y(x,t) = \frac{B}{\alpha A^{1/\alpha}} x^{1/\alpha-1} f_\alpha\left(x/x_{tip}(t)\right)\,, \tag{2}$$

where

$$f_\alpha(s) = \int_s^1 du \frac{1}{u^{1/\alpha-1}\sqrt{1-u^4}}\,. \tag{3}$$

The crucial step in determining the exponent α is the assumption that *velocity selection of the finger tip is governed by the anisotropy of surface tension* as in dendritic growth, which leads to the requirement

$$\rho^2 V = \text{const}\,, \tag{4}$$

where ρ is the radius and V the velocity of the tip. Because $V \sim dx/dt \sim t^{\alpha-1}$ and $\rho \sim \left(d^2x/dy^2\right)^{-1}|_{x=x_{tip}} \sim t^{2-3\alpha}$, this condition immediately leads to $\alpha = \frac{3}{5}$.

Let us return to noiseless DLA. This aggregation model is implemented by assigning counters to each perimeter site of the cluster, in which mass is accumulated *continuously* according to the DLA growth probabilities [16–18] and a growth event occurs each time a counter reaches the value corresponding to the mass of one particle. This is a deterministic growth model which, besides being interesting in its own right, also gives a reasonable description of cluster shapes observed in *noise-reduced* DLA during their compact-growth phase (whose duration increases with the noise-reduction threshold m).

When the number N of aggregated particles is interpreted as time, noiseless DLA on a square lattice is a Laplacian growth process with constant-flux boundary conditions at infinity and fourfold anisotropy imposed by the underlying lattice. Thus we ought to be able to construct a continuum description from the same ingredients as Almgren *et al.* Equations (1)–(3) should continue to hold. There is *no surface tension*, however, so we cannot expect Eq. (4) to be valid. But it is easy to guess at a substitute. What surface tension does in the Hele-Shaw problem is to provide a microscopic cutoff for interface fluctuations. In noise-reduced DLA, this cutoff is given by the lattice constant and noise reduction essentially serves as an amplifier of lattice anisotropy. Therefore, it is tempting to conjecture that again the (anisotropy of the) *small-length cutoff is responsible for shape and velocity selection in noiseless DLA*, and the most natural assumption for the tip radius is then

$$\rho \sim \text{const}\,, \tag{5}$$

where the constant should be on the order of the lattice constant. Of course, we know from extensive numerical simulations of both noise-reduced [9] and noiseless [16–18] DLA that the arm tips look sharp on length scales that are much larger than the lattice constant, which once more suggests that (5) holds true.

An immediate consequence of (5) is $\alpha = \frac{2}{3}$. We mention in passing that this is an upper limit for *growth processes*, because larger values of α would mean *decreasing* tip radii. The true range of α is thus $\frac{1}{2} \leq \alpha \leq \frac{2}{3}$ [19]. Expanding formula (2) with $\alpha = \frac{2}{3}$ about the tip, we obtain

$$x_{tip} - x = \left(\frac{2}{3}\right)^2 \left[\frac{A^3}{B^2} y^2 + \frac{2A^3}{27B^2} \frac{y^4}{At^{2/3}} + O\left(t^{-4/3}\right)\right] , \tag{6}$$

which relates the tip radius ρ to the two yet unknown constants A and B:

$$\rho = \frac{9B^2}{8A^3} . \tag{7}$$

Clearly, we can map the time scale on the particle number N by calculating the total cluster area

$$Na^2 = 8 \int_0^{x_{tip}} dx\, y(x,t) = 2\pi B t . \tag{8}$$

(The second equality in this equation holds for arbitrary α.) Using Eqs. (6) and (8), we can write

$$x_{tip}(N) = \frac{a}{2} \left[\frac{3}{2\pi} \left(\frac{a}{\rho}\right)^{1/2} N\right]^{2/3} , \tag{9}$$

$$y(x,N) = a \left[\frac{3}{2\pi} \frac{\rho}{a} N\right]^{1/3} \sqrt{\frac{x}{x_{tip}}}\, f\left(\frac{x}{x_{tip}}\right) , \tag{10}$$

where

$$f(s) = \int_s^1 du\, \frac{1}{u^{1/2}(1-u^4)^{1/2}} , \tag{11}$$

which eliminates all free parameters but ρ from the equations. Now there is definitely no microscopic theory that would allow us to determine ρ in a similar fashion as the constant on the right-hand side of the selection criterion (4) when surface tension provides the small-length cutoff. So it seems that the tip radius can only be found by fitting to numerical simulations. We shall, however, see that this is unnecessary, in a sense. In fact, since each cluster is grown from a one-particle seed, a least-biased guess would be that Eq. (9) continues to hold for this minimum cluster size, which provides $x_{tip}(N=1) = a/2$, determining ρ unambiguously:

$$\rho = \left(\frac{3}{2\pi}\right)^2 a \approx 0.228\, a ; \tag{12}$$

hence

$$x_{tip}(N) = \frac{a}{2} N^{2/3} , \tag{13}$$

$$y(x,N) = \frac{3}{2\pi} a N^{1/3} \sqrt{\frac{x}{x_{tip}}}\, f\left(\frac{x}{x_{tip}}\right) . \tag{14}$$

Figure 1 compares the shape described by (13) and (14) with clusters of various sizes. Obviously, the overall agreement is quite good. Even more impressive is a comparison of the armlengths L/a of a few simulated clusters with x_{tip}/a as calculated from Eq. (13), which is given in Table I.

For the first two clusters, the agreement is better than 1%. The three larger clusters have already started to develop sidebranches due to the influence of the outer circular boundary in the simulation (for an explanation of this effect see [18]); nevertheless, even in these cases the discrepancy does not get worse than roughly 2%.

Of course, the description by Eq. (14) must fail close to the origin of the coordinate system, simply because it predicts an overlap of the four petals of the cluster, which is a consequence of the infinite slope due to the square root in the shape expression. Since in the region where Eq. (14) is to be valid the inequality $y(x,t) \leq x$ must be satisfied, an estimate for the lower bound x_ℓ of this region follows from setting $y(x_\ell,t) = x_\ell$, which yields

$$\frac{x_\ell}{a} = \frac{9}{2\pi^2} \left[f\left(\frac{x_\ell}{x_{tip}}\right)\right]^2 . \tag{15}$$

For large N, the right-hand side can be approximated by the function value at $x = 0$, which shows that x_ℓ approaches a finite limit

$$\frac{x_\ell}{a} \underset{N\to\infty}{\longrightarrow} \frac{9}{32\pi} \left[\frac{\Gamma(\frac{1}{8})}{\Gamma(\frac{5}{8})}\right]^2 \approx 2.47 , \tag{16}$$

where we have used $f(0) = \frac{1}{4}\Gamma(\frac{1}{8})\Gamma(\frac{1}{2})/\Gamma(\frac{5}{8})$. Thus the relative range of validity of our continuum approximation increases with time, as $x_\ell/x_{tip} \to 0$ for $N \to \infty$.

Let us examine next what predictions we can make about the step lengths in the stable needle staircase near the cluster tip discussed by Batchelor and Henry [16]. First note that an expansion of (2) near the tip yields

$$y = \frac{B}{\alpha A^{1/\alpha}} (x_{tip} - x)^{1/2}\, x_{tip}^{1/\alpha - 3/2} + O\left(x_{tip}^{1/\alpha - 5/2}\right) , \tag{17}$$

so the very existence of a stable staircase requires $\alpha = \frac{2}{3}$; otherwise y would remain time dependent in the vicinity of the tip and the step lengths would not approach

TABLE I. Cluster armlengths: simulation (L/a) and theory ($x_{\rm tip}/a$).

N	L/a	$x_{\rm tip}/a$
4273	132	131.66
8757	211	212.43
18625	344	351.32
30109	473	483.91
53217	698	707.41

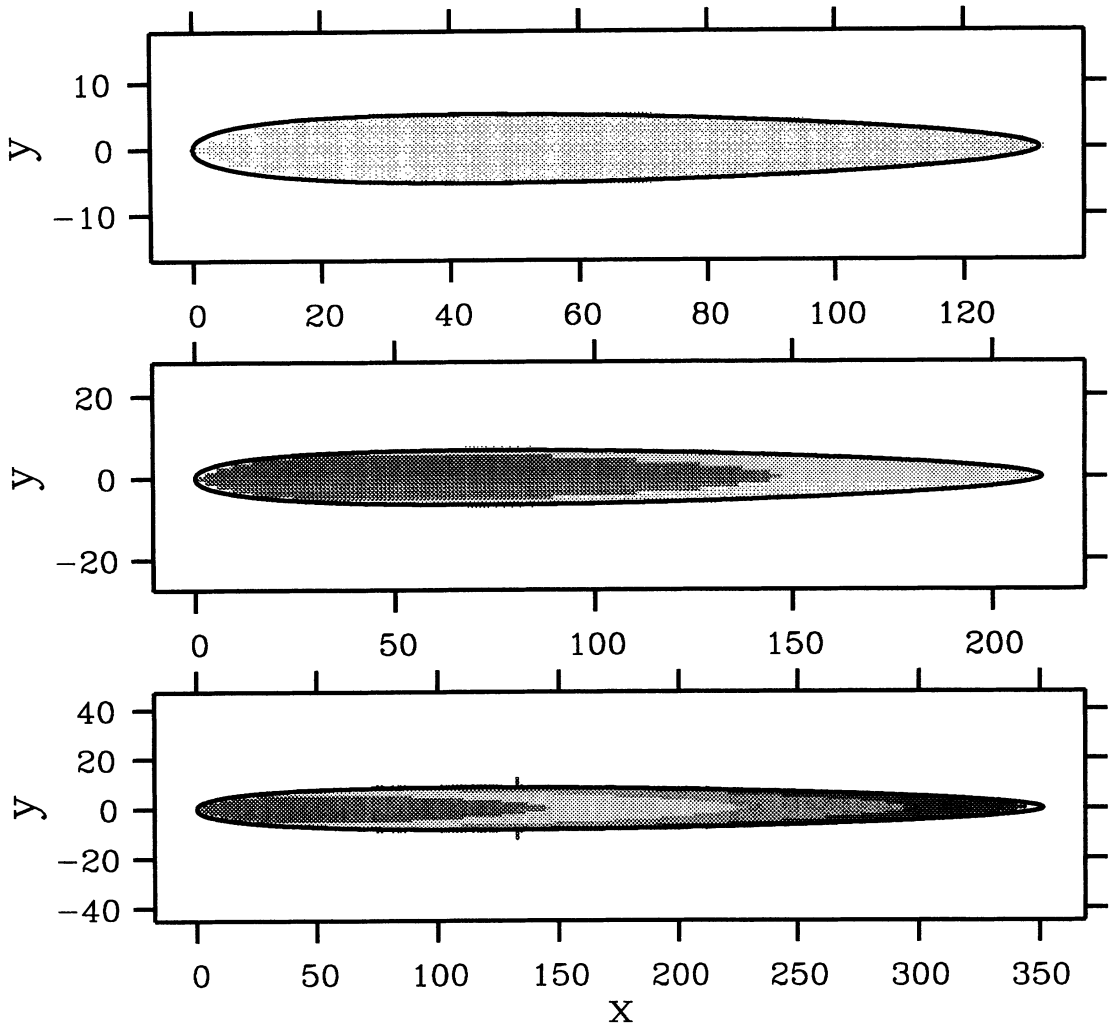

FIG. 1. Comparison of cluster shapes with the analytic prediction Eqs. (13) and (14). The cluster arms are represented as collections of squares, while the shape from continuum theory is given as unbroken lines. Particle numbers in the clusters from top to bottom: $N = 4273$, $N = 8757$, and $N = 18625$.

time independent values. Constancy of the tip radius ρ is therefore equivalent to the existence of a stable staircase.

Denote by x_k the position of the ledge of the kth step from the tip ($x_0 = x_{tip}$); then the staircase must asymptotically satisfy

$$a \sim y(x_k) - y(x_{k-1}) \quad (k \gg 1) . \tag{18}$$

Figure 2 shows a closeup of the tip region of the second cluster from Fig. 1 together with the approximating continuous contour. Observe that near the tip, the intersection points of the contour with the steps have distances slightly less than a in the y direction, i.e., the asymptotics (18) are not quite satisfied by the computed shape.

Inserting Eq. (18) into the parabolic profile, Eq. (6), we get an asymptotic recursion relation for the step lengths $\ell_k = (x_{k-1} - x_k)/a$,

$$\ell_k \sim \left(\frac{2a}{\rho} \sum_{i=1}^{k-1} \ell_i \right)^{1/2} \quad (k \gg 1, x_{tip} - x_k \ll x_{tip}) . \tag{19}$$

The lowest-order solution to this recursion relation is $\ell_k \sim k\, a/\rho$ ($k \gg 1$). If we assume (18) to hold for *all* k, we obtain $x_k = x_{tip} - (k\,a)^2/(2\rho)$ and thus

$$\ell_k = \frac{a}{2\rho} (2k - 1) . \tag{20}$$

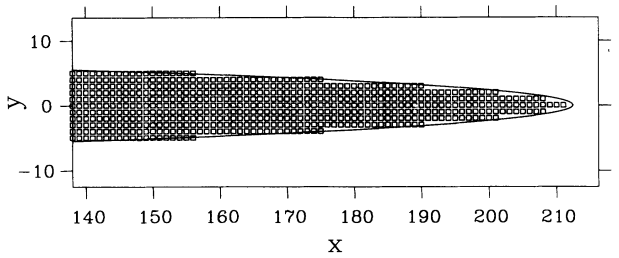

FIG. 2. Magnification of the tip region of the second cluster from Fig. 1. Note that at the position of the first step, the continuum shape $y(x) \approx \frac{3}{2}a$, i.e., the step barely intersects the contour. For the following steps, the intersection point moves downward along the ledge.

For small values of k, both formulas do not agree too well with the step lengths obtained numerically (see Table II). To understand this in more detail, let us obtain the step sequence via a different approach.

Rather than using the *geometric* relation (18) we use *dynamic* information to compute the staircase. According to Batchelor and Henry [16], if we number the perimeter sites starting with 0 at the tip, the growth probabilities along the staircase should satisfy

$$\sum_{i=1}^{\ell_1+\ell_2+\cdots+\ell_n-1} p_i < np_0 < \sum_{i=1}^{\ell_1+\ell_2+\cdots+\ell_n} p_i \,. \tag{21}$$

This immediately translates into an integral formulation for the continuum model

$$\int_{x_n}^{x_{tip}} p(x)\,dx = \left(n+\frac{1}{2}\right) p_0 \,, \quad n = 1,2,3,\ldots \,, \tag{22}$$

where p_0 is the tip growth probability or growth rate, while $p(x) = (1/a^2)dy/dN$ is the growth probability density along the cluster arm. The $\frac{1}{2}$ on the right-hand side of (22) accounts for the tip itself.

Both (21) and (22) state that per time unit the same mass is accumulated on each step, which is intuitively clear, if the step lengths are to be stable. Next we need an estimate for p_0 to utilize Eq. (22) and calculate the x_n. To this end, we divide the total growth rate, integrated from the position x_m of the maximum of $y(x)$ to the tip, by the number of steps, which is y_{max}/a. We then have

$$p_0 \approx \frac{a}{y_{max}} \int_{x_m}^{x_{tip}} dx\, p(x) \,. \tag{23}$$

Herein, x_m is given by $x_m = s_m x_{tip}$, where s_m is the solution of $s_m^{1/2}/(1-s_m^4)^{1/2} - \frac{1}{2}f(s) = 0$ and $y_{max} = 3\,a\,s_m N^{1/3}/[\pi(1-s_m^4)^{1/2}]$. Numerically, one obtains $s_m \approx 0.336$. Integrating $p(x)$ analytically, we find

$$p_0 = \frac{(1-s_m^4)^{1/2}}{12 s_m}\left(\frac{\pi}{2} - \arcsin s_m^2\right) N^{-1/3} \equiv \mu N^{-1/3} \,. \tag{24}$$

From this equation, we get a numerical value for the prefactor $\mu = 0.359$.

The positions of the step ledges are then given by $x_k = s_k x_{tip}$, where

$$s_0^2 = \sin\left(\frac{\pi}{2} - 2\pi\mu N^{-1/3}\right) \,, \tag{25}$$

$$s_k^2 = \sin\left(\arcsin s_{k-1}^2 - 4\pi\mu N^{-1/3}\right) \,, \quad k = 1,2,3,\ldots \,. \tag{26}$$

Only the second equation describes step positions, whereas the first corresponds to the tip itself, which must occupy a finite-length interval about x_{tip} in a continuum model (i.e., $x_0 < x_{tip}$ here). Expanding for large N, we arrive at

$$\ell_0 = 0.5\pi^2\mu^2 \,, \tag{27}$$

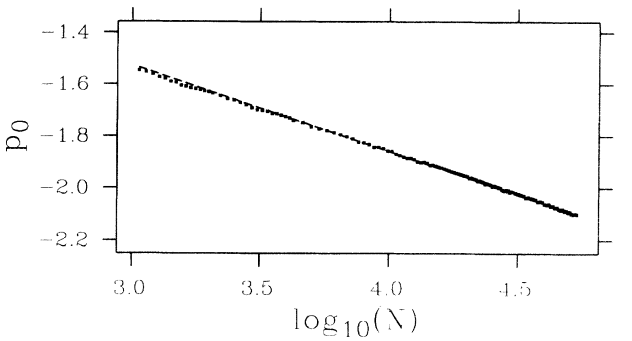

FIG. 3. Tip growth rate p_0 versus cluster size. The dashed line is a least-squares fit of the form $p_0 = \mu N^{-1/3}$, providing $\mu = 0.300$.

$$\ell_k = 2\pi^2\mu^2 + 2\pi\mu\left(2\sum_{i=0}^{k-1}\ell_i\right)^{1/2} \,. \tag{28}$$

Since the asymptotics of Eq. (28) must be just Eq. (19), we have another way to predict μ and hence p_0: $\mu = (a/\rho)^{1/2}/(2\pi) = \frac{1}{3}$. The two predictions of μ had better be close to each other, and indeed they are, to within 7 %.

Furthermore, we have compared these analytic results with numerical simulations, where we can measure the tip growth rate directly. Figure 3 is a double logarithmic representation of the numerical p_0 as a function of cluster size. Also shown is a fit of the functional relation $p_0 = \mu N^{-1/3}$ to the data. The obtained value $\mu = 0.300$ is lower than the analytic estimates, but the deviation is less than 20%, which appears reasonable for a continuum approximation that cannot exactly model the tip shape.

Table II contains a numerical comparison of the step lengths obtained from Eqs. (20) and (28) with the true step lengths observed in the simulation. For Eq. (20) and for Eq. (28) with $\mu = \frac{1}{3}$, the general agreement is reasonable though not impressive, except for the value of ℓ_1, which is completely off the mark. If the *measured* value of μ is taken in Eq. (28), the agreement is pretty good for all step lengths. The comparison is limited to $k \le 7$, because clusters for which the eighth step has already become stable have yet to be grown.

To conclude, we have shown that a continuum description of noiseless DLA is obtained from a condition Eq. (5) which, in complete analogy with the selection cri-

TABLE II. Comparison of numerical step lengths with various analytic expressions.

k	l_k (numerical)	l^k [Eq. (20)]	l_k [Eq. (28)] $\mu = \frac{1}{3}$	l_k [Eq. (28)] $\mu = 0.300$
0			0.55	0.44
1	3 – 4	2.19	4.39	3.55
2	7 – 8	6.58	8.77	7.11
3	10 – 11	10.97	13.16	10.66
4	14 – 15	15.35	17.55	14.21
5	18 – 19	19.74	21.93	17.77
6	22 – 23	24.13	26.32	21.32
7	25	28.51	30.71	24.87

terion (4), determines the growth exponent α and, once the constant on the right-hand side of the equation is specified, the tip velocity dx_{tip}/dN. Other than in the Hele-Shaw case, there is no microscopic theory available that would determine the constant, e.g., from a nonlinear eigenvalue problem. However, the form of the equation for the tip position [Eq. (9)], together with our knowledge of the initial condition, suggests an educated guess, which leads to a surprisingly satisfactory description. From this parameter-free theory, we obtain quantitative results for the tip position that are accurate in the percent regime. Moreover, the width of a cluster arm, the step lengths in the vicinity of the tip, and the tip growth rate can be estimated with decent accuracy. Because the step lengths are reproduced more accurately with $\mu = 0.300$ than with $\mu = \frac{1}{3}$, one might think that the actual value of ρ/a should exceed $(3/2\pi)^2$; however, this corrected value turns out to describe the total arm lengths worse than the chosen value. This small discrepancy is due to the facts that the needle shape employed in calculating the growth rates is not exact and that the continuum approximation can only imperfectly model the tip shape.

The most important outcome of our small exploration may be the demonstration that noiseless DLA belongs into a universality class that is *different* from that of dendritic growth or viscous fingering, since we obtain a different growth exponent α. In effect, this unambiguously answers the question—in the negative—whether noise reduction may be considered a way to simulate surface tension.

[1] T. A. Witten and L. M. Sander, Phys. Rev. Lett. **47**, 1400 (1981).
[2] T. A. Witten and L. M. Sander, Phys. Rev. B **27**, 5696 (1983).
[3] L. Pietronero, A. Erzan, and C. Evertsz, Phys. Rev. Lett. **61**, 861 (1988); Physica A **151**, 207 (1988).
[4] T. C. Halsey and M. Leibig, Phys. Rev. A **46**, 7793 (1992); T. C. Halsey, Phys. Rev. Lett. **72**, 1228 (1994).
[5] C. Tang, Phys. Rev. A **31**, 1977 (1985).
[6] J. Kertész and T. Vicsek, J. Phys. A **19**, L257 (1986).
[7] G. Rossi, Phys. Rev. A **34**, 3543 (1986); **35**, 2246 (1987).
[8] P. Meakin, Phys. Rev. A **33**, 1984 (1986).
[9] J.-P. Eckmann, P. Meakin, I. Procaccia, and R. Zeitak, Phys. Rev. A **39**, 3185 (1989).
[10] M. Cates, Phys. Rev. A **33**, 5007 (1986).
[11] K. Kassner, Phys. Rev. A **42**, 3637 (1990).
[12] J. Krug, K. Kassner, P. Meakin, and F. Family, Europhys. Lett. **24**, 527 (1993).
[13] R. Almgren, W.-S. Dai, and V. Hakim, Phys. Rev. Lett. **71**, 3461 (1993).
[14] E. Brener, Phys. Rev. Lett. **71**, 3653 (1993).
[15] K. Kassner and F. Family, Phys. Rev. A **39**, 4797 (1989).
[16] M. T. Batchelor and B. I. Henry, Physica A **187**, 551 (1992).
[17] C. Moukarzel, Physica A **188**, 469 (1992).
[18] K. Kassner, Fractals **1**, 205 (1993).
[19] H. Kesten, J. Phys. A **20**, L29 (1987).

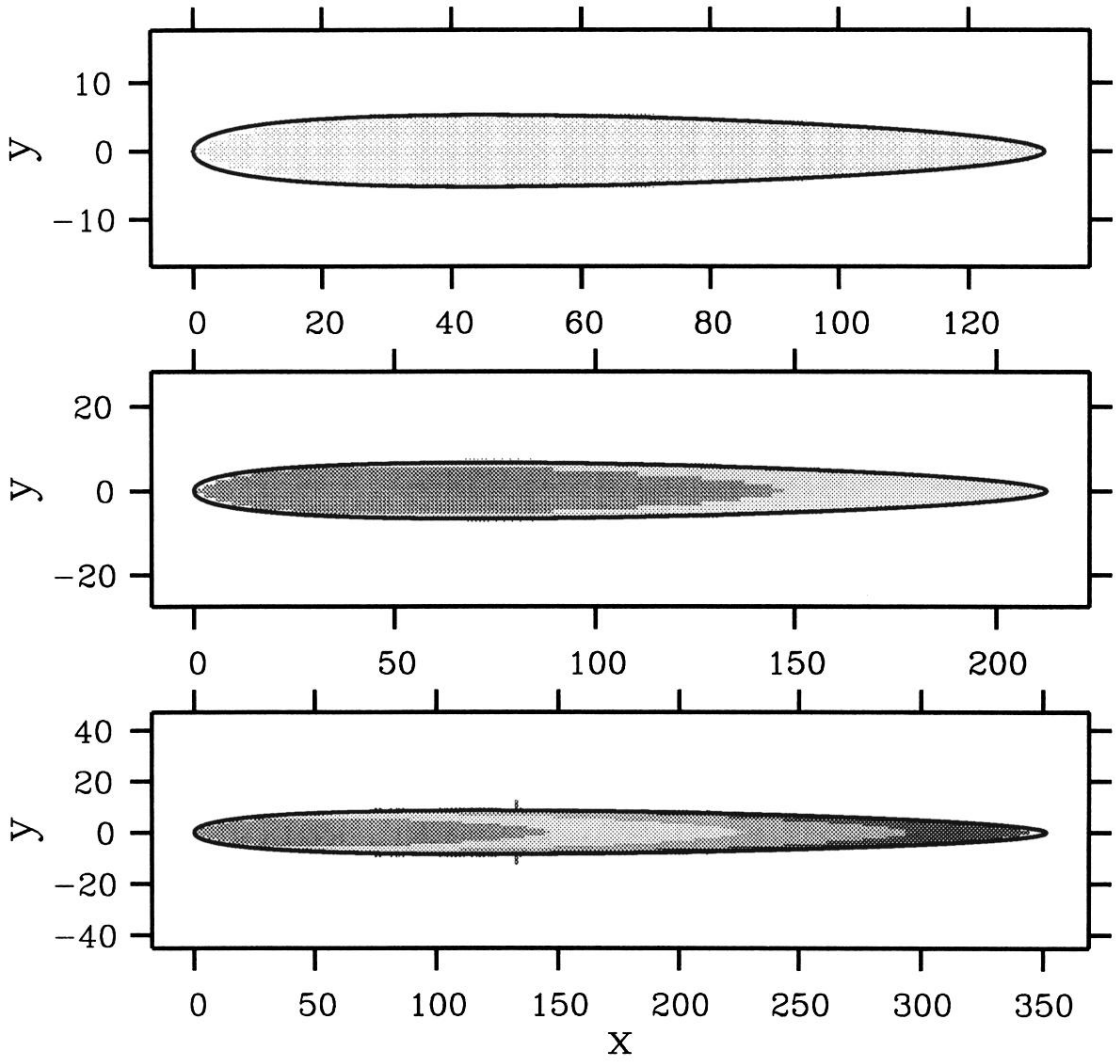

FIG. 1. Comparison of cluster shapes with the analytic prediction Eqs. (13) and (14). The cluster arms are represented as collections of squares, while the shape from continuum theory is given as unbroken lines. Particle numbers in the clusters from top to bottom: $N = 4273$, $N = 8757$, and $N = 18625$.